Molecular insight on unusually high specific hydrogen adsorption over silicon carbide

Yaremov, Pavel S.; Shcherban, Nataliya D.; Aho, Atte; Murzin, Dmitry

Published in:
International Journal of Hydrogen Energy

DOI:
10.1016/j.ijhydene.2019.01.081

Published: 01/01/2019

Document Version
Accepted author manuscript

Document License
CC BY-NC-ND

Molecular insight on unusually high specific hydrogen adsorption over silicon carbide

Pavel S. Yaremov[1], Nataliya D. Shcherban[1], Atte Aho[2], and Dmitry Yu. Murzin[2*]

[1] L.V. Pisarzhevsky Institute of Physical Chemistry, National Academy of Sciences of Ukraine, 31 pr. Nauky, Kiev, 03028, Ukraine

[2] Johan Gadolin Process Chemistry Centre, Åbo Akademi University, Biskopsgatan 8, 20500 Åbo/Turku, Finland

* Corresponding Author. E-mail address: dmurzin@abo.fi,

tel. + 358 2 215 4985, fax +3582215 4479 (Dmitry Yu. Murzin).

Abstract

Hydrogen adsorption over silicon carbide of different nature was investigated. High specific hydrogen adsorption (up to 15 μmol/m^2), nontypical for silicon carbide was obtained for the materials prepared by the template method. A more perfect truly "carbide" structure (with a higher content of Si–C bonds in the form of carbide) in this type of materials contributes to an increase of the specific hydrogen adsorption. However, some non-stoichiometricity manifested in the presence of carbon in other (non-carbide) bonds (graphite or terminal and sp^3 hybridized C) is required for exceptionally high specific hydrogen adsorption. The influence of the adsorbate nature for several gases (H_2, N_2, CO) was found to be less prominent for SiC compared to carbon and silica materials. This feature inherent only to silicon carbide exhibiting an increased level of specific hydrogen adsorption, is due to cooperative adsorption, accompanied by an abnormally high loading of the adsorbent surface in the supercritical region.

Keywords: silicon carbide; template method; specific hydrogen adsorption; cooperative adsorption; semiconductor adsorbent; microdefects; supercritical temperature region.

1. Introduction

Hydrogen storage has attracted attention of researchers due to the fact that hydrogen, unlike traditional fuel resources, is an environmentally friendly fuel, which allows to solve both energy and environmental problems simultaneously [1, 2]. While a long time, carbon nanotubes (CNT) were considered as promising hydrogen adsorbents, their main disadvantage is a low interaction energy with hydrogen (ca. 1 kcal/mol). The main approach to increase the interaction energy between hydrogen and the adsorbent surface is introduction of point charges into its structure. This can be done by doping with heteroatoms or by incorporation of light metal atoms, which eventually induce appearance of dipole interactions [1]. This approach led to many studies of hydrogen storage by adsorbents of other nature, in particular, boron nitride [3, 4] and even more promising silicon carbide [5–7].

An increased hydrogen adsorption over silicon carbide compared with materials of other nature, in particular carbon, is confirmed by both experimental studies [8–11] and theoretical calculations [7, 12–14]. Such behavior was related to a partially heteropolar binding nature of SiC bonds. Point charges present on the walls of silicon carbide nanotubes can induce dipoles on the hydrogen molecules (polarization centers), which leads to more efficient hydrogen binding [7].

Use of porous materials with semiconducting properties, in particular SiC, is also due to ability of adsorbed molecules of hydrogen to capture a free electron or a free hole, herewith passing from an electroneutral to a charged state. At the same time, an electron or a hole captured by an adsorbate are involved in the formation of a chemisorption bond and increases adsorption capacity of the surface to hydrogen. Charge carriers (electrons and holes) on the microdefects of the surface formed by impurities in the semiconductor framework [15–17] can also act as the adsorption sites.

One of the promising approaches to create effective sorbents for hydrogen storage is preparation of porous materials, in particular silicon carbide based ones, by template synthesis methods [18, 19]. Variation of the process conditions (pyrolysis), the precursors nature and the type

of silica template allows regulation in a wide range of the porous structure (volume and pore size, specific surface area) and the surface nature of the obtained materials. This allows an increase of their adsorption capacity in general and, in particular, adsorption specificity towards hydrogen, namely energy and specific adsorption of H_2, due to formation of adsorption sites with an electron and hole nature.

While SiC nanotubes for H_2 adsorption have been reported in the literature [7–10, 12–14], they have several limitations such as high price and low porosity, therefore determination of hydrogen adsorption over porous SiC materials different from nanotubes is an important task.

The aim of this work was to clarify a relationship between the structure of silicon carbide and sorption properties towards nitrogen, hydrogen and carbon oxides. Identification of the factors influencing the specific adsorption of hydrogen and other gases, in particular carbon oxides, in the supercritical temperature region compared with a standard adsorbate (nitrogen), for silicon carbide of different structures, as well as other types of adsorbents (silica and carbon) was thus in the focus of this study.

2. Material and methods

2.1. Sample preparation

The sample coded as SiC-bulk-sucr was prepared from a mixture of sucrose (Ecolab, Ukraine) and silica (Aerosil A-175, Chlorovinyl Co, Kalush, Ukraine) with the sucrose/silica weight ratio of 3. The corresponding mixture was heated at 1673 K (heating rate 2 K/min) in an inert atmosphere for 9 h. SiC-bulk-sucr-HF was obtained after stirring of SiC-bulk-sucr in 15% HF (Merck) water solution overnight followed by washing with distilled water and drying at 373 K. SiC-bulk-C was synthesized from a mixture of carbon (carbonized sucrose at 1173 K for 2.5 h) and silica (Aerosil 175), the carbon to silica mass ratio was equal to unity (the heating was performed using the above mentioned temperature mode).

SiC-SBA-3, SiC-SBA-15, SiC-KIT-6 and SiC-MCF were prepared via the template method using initial mesoporous silicas of several types (SBA-3, SBA-15, KIT-6, MCF, respectively) obtained by conventional methods [20]. Synthesized silica templates after calcination (823 K for 5 h in air) were used to produce carbon-silica composites via carbonization of sucrose in the pores of mesoporous molecular sieve (MMS) in the presence of H_2SO_4 (98%, Macrochem) as a catalyst. For this purpose, a weighed amount of initial mesoporous silica was impregnated with an aqueous solution containing a certain amount of sucrose and sulfuric acid, dried primarily at 373 K for 6 h followed by heating for another 6 h at 433 K. The resulting mixtures were again mixed with an aqueous solution of sucrose and sulfuric acid. The resulting dark brown powder obtained after repeated treatment in similar conditions was heated (5 K/min) in an inert atmosphere (argon) to 1173 K and kept at this temperature for 2.5 h. The synthesized carbon-silica composites were heated at 1673 K (heating rate 2 K/min) in an inert atmosphere for 9 h. The resulting powders were purified by heating to 973 K in air and washing in HF water solution to remove the residual carbon and silica respectively. The purified powders had a gray color.

The silica component was removed by treatment of a part of carbon-silica composite based on SBA-15 and KIT-6 with 15% HF solution giving carbon materials CMK-3 and CMK-8, respectively. Carbons were filtered, washed with ethanol and dried at 373 K.

SiC-nanoamor was purchased from NanoAmor and used without further treatment.

C_3N_4-bulk was synthesized via bulk pyrolysis of melamine according to the procedure previously published [21].

CN-SBA-15 was prepared using ethylenediamine and carbon tetrachloride as precursors and SBA-15 as a hard template according to [22].

2.2. Characterization

The phase composition of the samples was determined by powder X-ray diffraction. The computerized Bruker D8 Advance diffractometer was equipped with Cu K_α (λ = 0.15406 nm) X-ray source.

Adsorption isotherms of nitrogen, hydrogen, carbon monoxide and carbon dioxide (all of 99.99% purity) were measured by a volumetric method (up to 760 Torr) on Sorptomatic 1990. The specific surface area S_{BET} was evaluated using the BET equation [23]. Mesopore sizes were determined using the Barrett-Joyner-Halenda (BJH) method [24]. For products containing both micro- and mesopores, the values of micropore volume (V_{micro}) and the mesopore specific surface area (S_{meso}) were evaluated by using the comparative *t-plot* method [23]. Additionally, the initial adsorption potential $|\Delta\mu_0|$ was estimated using the method of excess surface work for determination of the specific surface area [25].

XPS-analysis of the samples was made using Perkin-Elmer PHI 5400 spectrometer with a Mg K_α X-ray source operated at 14 kV and 200 W. The pass energy of the analyzer was 17.9 eV and the energy step 0.1 eV. The charging was adjusted according to the C-C bond at 284.5 eV. Peak fitting was performed with the program XPS Peak 4.1. The background was corrected with the Shirley function. The sensitivity factors used in the quantitative analysis for C 1s and Si 2p were 0.296 and 0.339 respectively.

TEM-images were recorded on a transmission electron microscope TEM JEOL JEM-2100 under an accelerating voltage of 100 kV. Samples for TEM studies were grinded in an agate mortar with ethanol, the resulting suspension was applied on a copper mesh coated with a carbon film.

3. Results

3.1. XRD and nitrogen adsorption

In terms of the phase composition all SiC samples are β modification of silicon carbide, as evidenced by the presence of a strong reflex at $2\theta = 35.7^o$ (Fig. 1). A weak reflex at $2\theta = 33.7^o$ indicates

the presence of α-SiC as an impurity. A broad reflex at ca. 18° for SiC-nanoamor testifies presence of amorphous phases such as carbon or SiC_{1+x} [26]. A black color of this sample is an additional evidence of the impurities [26].

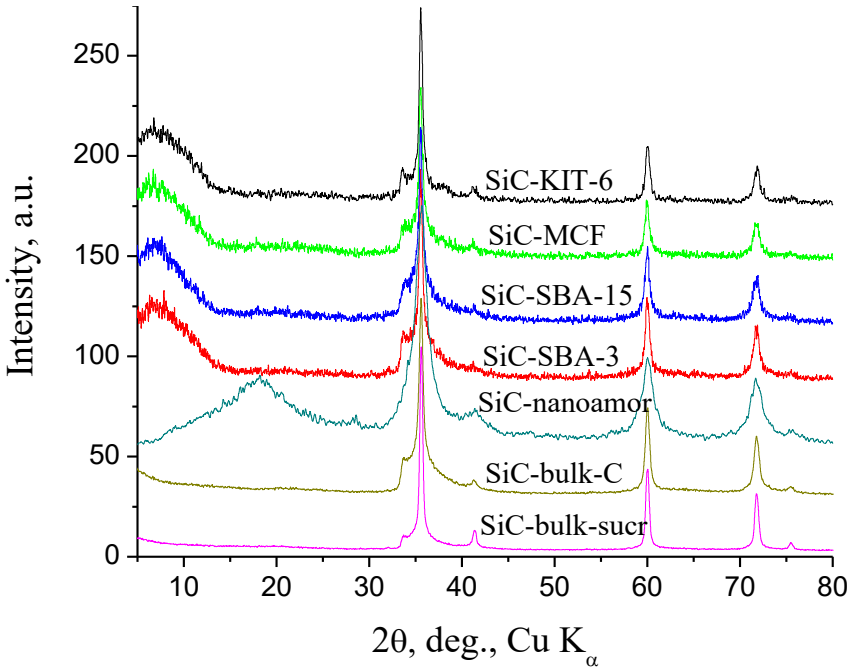

Fig. 1 – X-ray diffraction patterns of SiC samples.

Analysis of the nitrogen ad(de)sorption measurements (Table 1) shows that silicon carbide prepared by the bulk method (SiC-bulk-sucr) is characterized by a small specific surface area (35 m^2/g) and total adsorption up to ~ 0.1 cm^3/g (at $p/p_0 = 1.0$). Treatment of the obtained material with an aqueous solution of hydrofluoric acid results in a significant increase in texture characteristics, in particular, the total adsorption volume and specific surface area up to 0.71 cm^3/g and 120 m^2/g, respectively (sample SiC-bulk-sucr-HF). Utilization of porous carbon (the total pore volume of 0.3 cm^3/g and the specific surface area of 745 m^2/g) in a mixture with silica (aerosil A-175) contributes to the formation of mesoporous silicon carbide (sample SiC-bulk-C, V_{meso} = 0.31 cm^3/g, S_{meso} = 45 m^2/g). The commercial SiC-nanoamor is characterized by a significant nitrogen adsorption (up to 0.57

cm^3/g, the specific surface area 160 m^2/g) and contains pores larger than 20 nm. Silicon carbide prepared by the template method from carbon-silica composites is characterized by a developed surface (up to 410 m^2/g), a large total adsorption level (up to ~ 1.0 cm^3/g at $p/p_0 = 1.0$), a broad pore size distribution (in the range of 20 to more than 50 nm). Parameters of the porous structure of silicon carbide are to a certain extent determined by the adsorption characteristics of the used silica templates (Table 1), however, a clear correlation is observed for the carbon replicas of the corresponding templates [11, 27]. An increase of the mesopore volume and mesopore specific surface area in carbon replicas leads to an increase in the "interphase" space, in which the carbothermal processes of the formation and growth of SiC particles occur. As a result, mesoporosity of the carbon replicas determines the specific surface area of silicon carbide (Table 1).

Table 1 – Textural characteristics (N_2 ad(de)sorption, 77 K) of silicon carbide, prepared from carbon-silica composites via bulk and template (precursor – sucrose) methods (1673 K, Ar) using MMS type SBA-3, SBA-15, KIT-6 and MCF as templates.

Sample	V_{micro} [1)], cm^3/g	V_{meso}, cm^3/g	S_{meso} [1)], m^2/g	D_{max}, nm	S_{ext} [1)], m^2/g	S_{BET}, m^2/g	V_{Σ} [3)], cm^3/g	$\lvert\Delta\mu_o\rvert$, kJ/mol
Initial silica templates								
SBA-15	0.06	0.90	425	6.8±0.3	55	630	0.96	11.5
KIT-6	0.10	1.22	550	7.4±0.3	45	830	1.32	12.5
Carbon materials								
CMK-3	0.11	1.07	730	3.6±0.3	130	1125	1.18	28.0
CMK-8	0.05	1.88	855	3.7±0.5 10.9±0.9 [2)]	535	1570	1.93	19.0
Silicon carbide								
SiC-bulk-sucr	–	*	15	19	20	35	0.085	4.6
SiC-bulk-sucr-HF	–	*	20	18	100	120	0.71	9.7

SiC-bulk-C	–	0.31	45	> 20	10	55	0.31	4.4
SiC-nanoamor	–	*	50	> 20	110	160	0.57	7.2
SiC-SBA-3	–	0.16	40	21	–	40	0.16	3.5
SiC-SBA-15	–	0.23	45	38	5	50	0.23	5.2
SiC-KIT-6	–	*	*	> 50	210	410	1.02	2.9
SiC-MCF	–	*	*	> 50	90	105	0.42	3.1

[1] – calculations using *t-plot* method;
[2] – mesopore diameter D_{max} calculated from adsorption isotherms branches using *BJH* method;
[3] – adsorption at $p/p_0 = 1.0$.
* – not determined.

3.2. Hydrogen adsorption

Adsorption properties of synthesized silicon carbide towards hydrogen (Fig. 2, Table 2) were analyzed taking into account characteristics of the porous structure obtained from the adsorption isotherms of the standard adsorbate – nitrogen, under the same conditions of ad(de)sorption for nitrogen and hydrogen (T = 77 K, p ≤ 760 Torr). For SiC the total adsorption capacity towards hydrogen is within the range of 0.08 – 1.24 wt.% at 77 K and 760 Torr. The maximum hydrogen adsorption values observed for SiC-KIT-6 with the maximum specific surface area (S_{BET} = 410 m^2/g) are in line with the porous structure of the synthesized materials (Table 1).

Comparison of hydrogen adsorption isotherms for silicon carbide and carbon (CMK-3) obtained on the basis of mesoporous silica SBA-15 (Fig. 3), indicates some general differences. In particular, a decrease of the hydrogen adsorption energy over silicon carbide (less steep initial sections of isotherms) and an absence of saturation at an equilibrium pressure of 760 Torr can be seen. Analysis of the calculated values of the initial hydrogen adsorption potential (Table 2) shows a significant decrease in the values of $\Delta\mu_{0H2}$ for silicon carbide samples compared to the corresponding carbon replicas (for CMK-3: $\Delta\mu_{0H2}$ – from 5.2 to 2.1 – 2.3 kJ/mol) and even to the initial silica templates (for Si-SBA-15: $\Delta\mu_{0H2}$ – 2.9 kJ/mol). Such differences in the hydrogen adsorption energy can be due to

changes in the chemical nature of the studied materials, in particular, a decrease in density of the adsorption sites on the surface – from carbon (length of the chemical bond >C=C< – 1.42 nm) to silica (≥Si–O– – 1.62 nm) and silicon carbide (≥Si–C≤ – 1.77 nm).

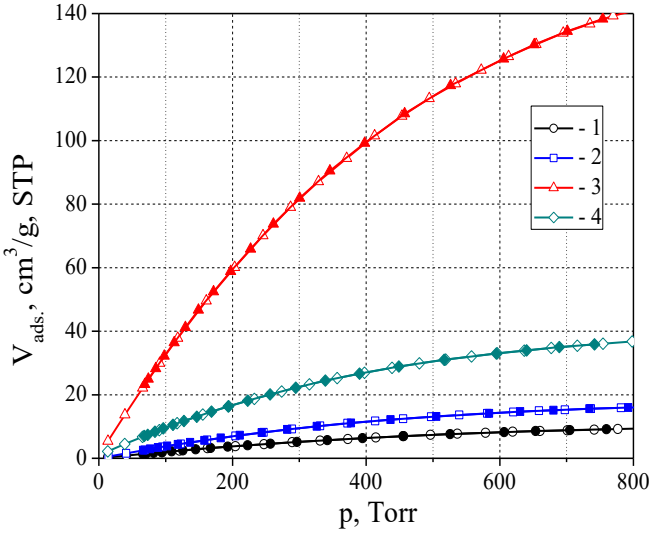

Fig. 2 – Hydrogen adsorption isotherms (77 K) for silicon carbide samples obtained by the template method in SBA-3 (1), SBA-15 (2), KIT-6 (3), MCF (4). Filled symbols – adsorption, empty symbols – desorption.

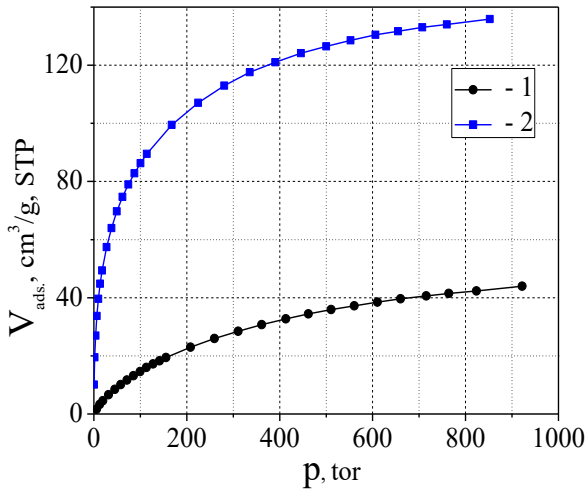

Fig. 3 – Hydrogen adsorption isotherms (77 K) for the initial template MMS type SBA-15 (1) and the corresponding carbon replica CMK-3 (2).

In order to characterize adsorption specificity of the silicon carbide surfaces towards hydrogen, the specific adsorption on the surface (S_{BET}) ρ_{H2} was calculated (at 760 Torr, Table 2). Analysis of the specific hydrogen adsorption indicates an unexpected significant increase in the ρ_{H2} values for synthesized silicon carbide samples (up to ~ 15 μmol/m^2), compared to silica (ρ_{H2} ~ 3 μmol/m^2) and even carbon (ρ_{H2} ~ 5 μmol/m^2) materials as it was found in our previous study [11].

Table 2 – Parameters of hydrogen adsorption at 77 K for samples of silica MMS, corresponding carbon materials and silicon carbide.

Sample	Hydrogen adsorption (p = 760 Torr)		Hydrogen adsorption potential $\lvert\Delta\mu_o\rvert$, kJ/mol
	a, wt.%	Specific adsorption on the pore surface (S_{BET}), μmol/m^2	
Initial silica templates			
SBA-15	0.37	3.0	2.9
KIT-6	0.50	3.0	2.8
Carbon materials			
CMK-3	1.20	5.3	5.2
CMK-8	1.70	5.4	4.2
Silicon carbide			
SiC-bulk-sucr	0.04	6.1	2.6
SiC-bulk-sucr-HF	0.16	6.6	2.5
SiC-bulk-C	0.19	15.2	2.4
SiC-nanoamor	0.43	13.8	2.1
SiC-SBA-3	0.08	10.3	2.1
SiC-SBA-15	0.14	14.7	2.2
SiC-KIT-6	1.24	15.1	2.2
SiC-MCF	0.32	15.0	2.3

4. Discussion

A higher adsorption capacity towards hydrogen for SiC nanotubes, compared to carbon nanotubes, might be associated with a larger Si–C bond length than for C–C (1.771 Å vs. 1.42 Å) [28] as well as a higher binding energy of the adsorbate due to a partially heteropolar nature of the Si–C bonds [7]. An increase in the adsorption capacity of materials toward hydrogen can occur as a result of an increase in the binding energy of hydrogen due to point charges on the adsorbent surface [7]. Higher hydrogen adsorption, in comparison with carbons, can be thus related to appearance of dipole interactions induced by the surface charges of silicon carbide. Such interactions provide an additional stabilization of hydrogen [14, 29], which is observed, in particular, for carbon nanotubes doped with alkali metal cations. This doping is accompanied by an increase in the hydrogen adsorption compared to undoped carbon nanotubes. Charge induced dipole interactions are a result of charge transfer from an alkali metal to the carbon tube and subsequent polarization of hydrogen. However, there are limitations for hydrogen adsorption capacity increase through creation of point charges on the adsorbent surface. Therefore, the reasons of an increase of hydrogen adsorption for silicon carbide should be related to other features of its structure, in particular, its semiconductor nature.

Adsorption and desorption of hydrogen over semiconductor surface are rather complex and not well understood, which is due to significant structural and electronic changes of the surface during adsorption [30]. As a rule, adsorption of hydrogen atoms is accompanied by the saturation of torn (unsaturated) bonds on semiconductor surfaces [30–32].

According to the electron theory of chemisorption [15–17], the chemosorbed molecule is a surface defect and can capture a free electron or a free hole, going from an electroneutral to a charged state. At the same time, the captured electron or the hole are involved in the chemisorption bond. Theoretical calculations have showed [15–17] that the total concentration of adsorption sites (free + occupied) in a semiconductor does not remained constant and is increased during adsorption as new adsorption sites are formed. The initial amount of adsorption sites depends on the Fermi level position

and, thereby, the concentration of the sites can be increased also by introduction into the crystal (or on its surface) particular additives which are shifting the Fermi level not participating at the same time in adsorption themselves [15–17].

Analysis of adsorption characteristics of synthesized silicon carbide materials shows that hydrogen adsorbed on the surface can be considered as the surface microdefects, since its presence disturbs the periodic structure of the surface. Such defects act as traps for free electrons or free holes (depending on the defect nature) acting as nuclei for their localization and in this way serving as newly formed sites of hydrogen adsorption. Such qualitative analysis of adsorption implies that in general a classical Langmuir adsorption isotherm should not hold for quantitative description of hydrogen adsorption data on silicon carbide and other models taking into account changes in the properties of adsorbents should be invoked. Numerical analysis of adsorption data using the Sips isotherm will be presented below. Such isotherm is capable of explaining experimentally observed S-shaped behavior during adsorption by considering generation of additional sites upon adsorption.

Despite a high energy of the initial hydrogen adsorption over a local site (complete hydrogen desorption for SiC is achieved only at $p \leq 10^{-4}$ Torr and a temperature above 623 K), which can also occur with dissociation, the total energy ($\Delta\mu_{0H2}$) is an apparent one. Such apparent character is stipulated by the fact that $\Delta\mu_{0H2}$ is calculated from an experimentally observed overall isotherm, which is influenced by a gradual change in the electronic nature of the surface, concentration of adsorption sites, etc. Absence of a noticeable adsorption-desorption hysteresis in isotherms, which is a typical feature of chemisorption, indicates a combined mechanism of hydrogen adsorption on the surface of synthesized SiC, comprising not only chemisorption with formation of additional H_2 adsorption sites and possibly physical adsorption at higher pressures.

High values of the specific hydrogen adsorption for silicon carbide obtained by the template method in comparison with the same materials synthesized by a traditional bulk method (SiC-bulk-sucr) and adsorbents with other nature (silica, carbon) are associated with the appearance of dipole

interactions and cooperative character of adsorption on semiconductor surface. Such features of SiC materials, determining their increased adsorption capacity towards hydrogen, should be related to the chemical nature of SiC surface, which was investigated by XPS (Fig. 4).

According to XPS (Fig. 4), the peak in the C1s region can be deconvoluted into two components, the main at ~282.8 eV corresponding to the carbon – silicon bond in the form of carbide SiC. A peak at 284.5 eV can be due to the presence of some excess carbon on the surface and thereby formation of graphite clusters [33, 34] or because of a special form of carbon acting as a terminal one for the SiC(0001) surface [35]. The third component at 285.7 eV for SiC-nanoamor corresponds to sp^3 hybridized carbon in the C–C bonds. The main component of the peak in the Si 2p region (Fig. 5) at the binding energy of 100.6 eV corresponds to the bond between silicon and carbon in silicon carbide, whereas a low intensity peak at 102.6 eV is assigned to bond between silicon and oxygen in silica [36, 37].

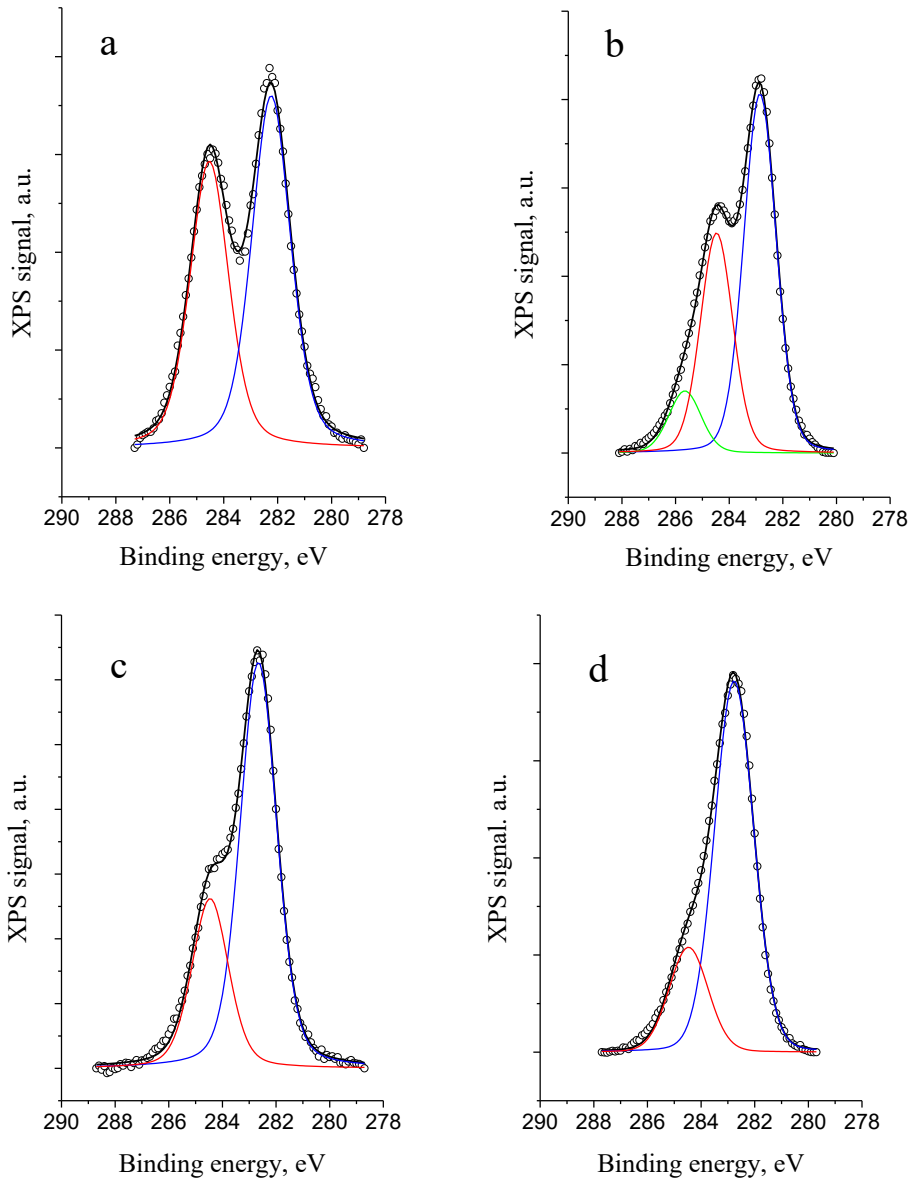

Fig. 4 – XPS spectra of the C 1s region for SiC-bulk-sucr (a), SiC-nanoamor (b), SiC-MCF (c) and SiC-KIT-6 (d).

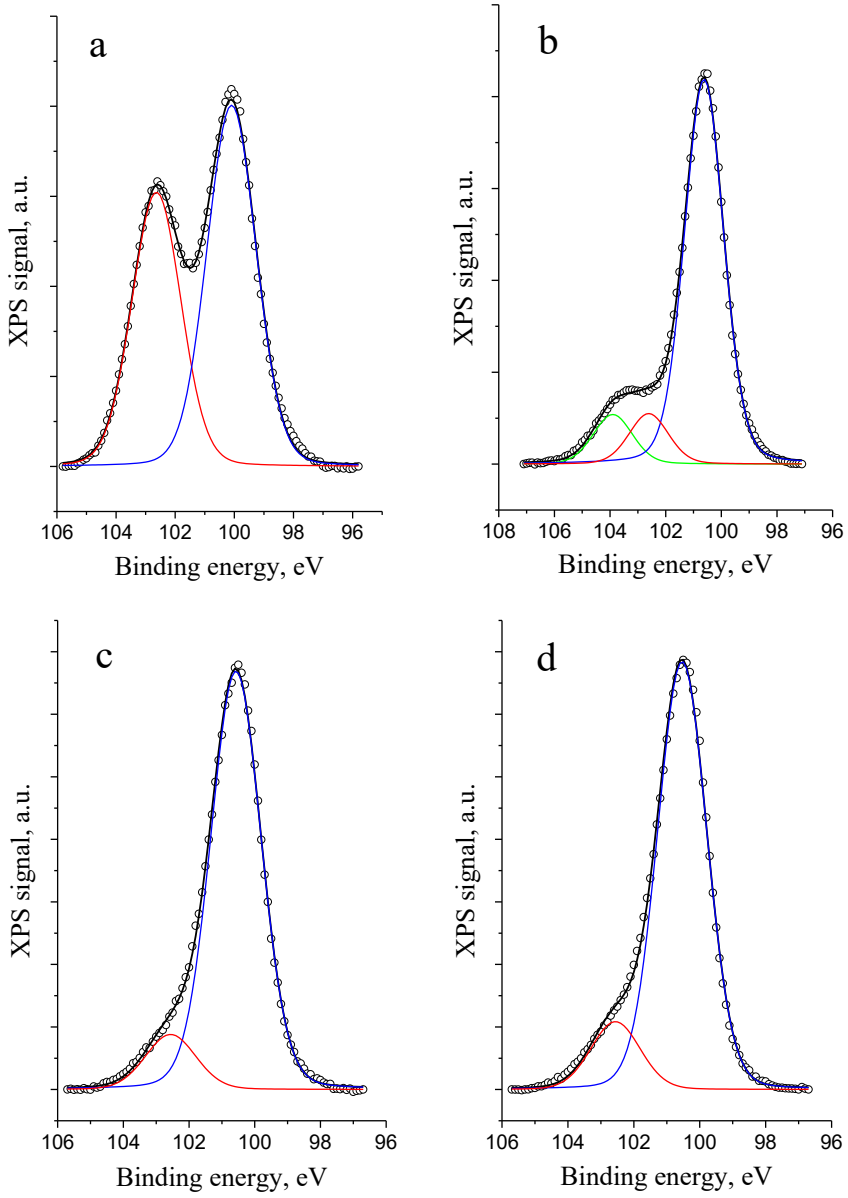

Fig. 5 – XPS spectra of the Si 2p region for SiC-bulk-sucr (a), SiC-nanoamor (b), SiC-MCF (c) and SiC-KIT-6 (d).

As can be seen from Fig. 4 and Table 3, the fraction of the peak corresponding to different forms of excess "non-carbide" carbon (graphite or terminal and sp^3 hybridized ones – peaks at 284.5 and 285.7 eV, respectively) is decreased from SiC-bulk-sucr (Fig. 4a) to SiC-KIT-6 (Fig. 4d). Simultaneously, there is an increase in the fraction of truly "carbide" carbon (peak at ~ 282.8 eV) in the specified samples from 55 to 78% (Table 3).

Table 3 – Percentage of different carbon-containing groups on the surface of silicon carbide according to XPS.

Sample	Contents of different C species on the adsorbent surface (%)		
	Si–C	C graphite/terminal	sp^3 C in C–C
SiC-bulk-sucr	55.3	44.7	-
SiC-nanoamor	56.0	34.3	9.7
SiC-MCF	70.5	29.5	-
SiC-KIT-6	78.0	22.0	-

Comparison of the obtained results with the adsorption data for hydrogen (Table 2) shows a correlation of the specific hydrogen adsorption with the fraction of carbon bound to silicon in the form of carbide SiC (Fig. 6). An increase in the content of the intrinsic carbide component is accompanied by a significant increase in the specific hydrogen adsorption (from 6 to 15 μmol/m^2). Maximal values of the specific hydrogen adsorption already for SiC-MCF and absence of a further increase for SiC-KIT-6 with a higher content of Si–C surface bonds should be noted. Thereby, in the studied series of materials, an increase in hydrogen specific adsorption is related to truly carbide Si–C bonds, which to a certain extent can characterize the degree of perfection of silicon carbide. Presence of a significant number of carbon formations of different nature, on the contrary, is accompanied by a decrease in the specific hydrogen adsorption to the values typical for carbon materials (Table 2). Typical values of specific hydrogen adsorption (c.a. 6 μmol/m^2) are observed for high-crystalline commercial samples of silicon carbide (Aldrich), obviously containing a high amount of the carbide component, likely due to a high synthesis temperature. Therefore, presence of a certain fraction of non-carbide carbon is necessary to achieve a high specific hydrogen adsorption. Such partial non-stoichiometric feature of silicon carbide, namely, an insignificant excess of the framework carbon atoms, which can serve as microdefects, and their concentration on the surface largely determine the level of the initial and the

total specific hydrogen adsorption. Presence of such microdefects is probably a reason of a significant difference in the values of specific hydrogen adsorption for the synthesized SiC samples (10 – 15 μmol/m^2) and chemically pure high crystalline commercial samples (up to 6 μmol/m^2, Table 2).

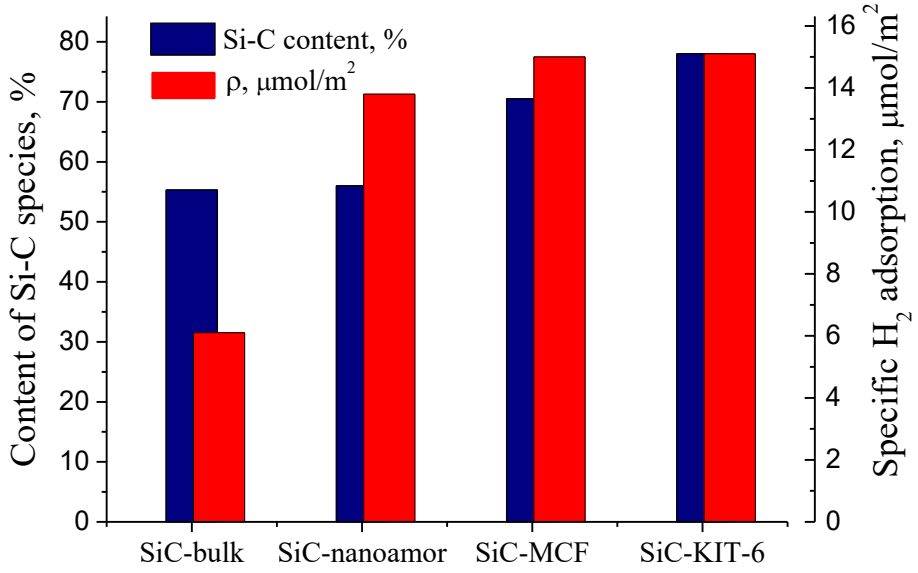

Fig. 6 – Content of carbide Si–C bonds and specific hydrogen adsorption for silicon carbide samples.

According to the TEM data (Fig. 7), the structure of silicon carbide, obtained by the template method, is characterized by a presence of packaging defects. Such defects can decrease the surface energy of SiC particles by limiting the growth of silicon carbide along the lowest surface energy crystal planes (111). Subsequently SiC structures with the packaging defects have a lower surface energy than materials without such defects [38]. The packaging defects acting as additional adsorption sites for hydrogen can be thus an additional reason for a high hydrogen adsorption capacity of the synthesized silicon carbide. Possibility of cooperative adsorption of hydrogen and other gases on the surface of SiC is due both to the chemical nature of the surface and to a certain extent, a relatively high level of initial gases adsorption (chemisorption), which depends on the presence of chemical and structural surface defects.

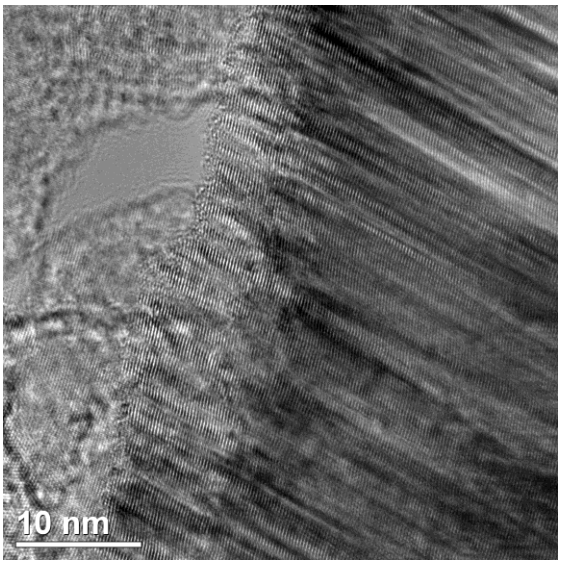

Fig. 7 – TEM image of SiC-SBA-15.

The obtained results open a possibility of a significant increase in the adsorption capacity of porous semiconductor materials towards hydrogen, in particular on the basis of silicon carbide.

Adsorption of gases on semiconductors

In order to explore adsorption of gases by semiconductors, in particular by carbon nitride, adsorption of hydrogen, nitrogen and carbon oxide was studied also in the supercritical conditions. Under such conditions a significant decrease of intermolecular interactions between adsorbates and an increase of interactions of adsorbates with the semiconductor surface are expected. For SiC and C_3N_4 in a region of low coverage (<0.1 μmol/m^2, 253 K, Figs. 8, 9), a pronounced gradual adsorption of gases (H_2, N_2, CO) is noticeable, apparently due to accelerated interactions of adsorbates with the semiconductor surface sites at elevated adsorbate pressures. At a lower adsorption temperature there is a significant increase in the adsorption potential while acceleration of adsorption is less pronounced (Table 3).

The S-shape behavior of adsorption visible from Figs. 8 and 9 was discussed in the literature using the Sips equation [39], which was originally derived assuming a Gaussian distribution of adsorption energy. The Sips isotherm is mathematically equivalent to the Hill adsorption isotherm frequently used in describing binding of substrates to enzymes, when due to cooperative effects such binding is accelerated upon an increase of substrate concentration. The Hill equation implies that the substrate binding ability at one site on the macromolecule (enzyme) can influence different binding sites on the same macromolecule [40].

While such approach has not been practically utilized for adsorption of gases on semiconductor surfaces there is a clear similarity between cooperative effects in enzymatic catalysts and in adsorption on semiconductors. While apparently the origin of both phenomena, from the formal viewpoint the same adsorption/binding isotherms can be applied, because, as discussed above, exposure of SiC or carbon nitride surfaces to, for example, hydrogen leads to creation of additional sites. Subsequently in the current work the Sips equation

$$\rho = \frac{\alpha_1 p^{\alpha_2}}{\alpha_3 + p^{\alpha_2}} \qquad (1)$$

was utilized for modelling the experimental data. In eq. (1) α_{1-3} are parameters, which were calculated by numerical data fitting using Origin software.

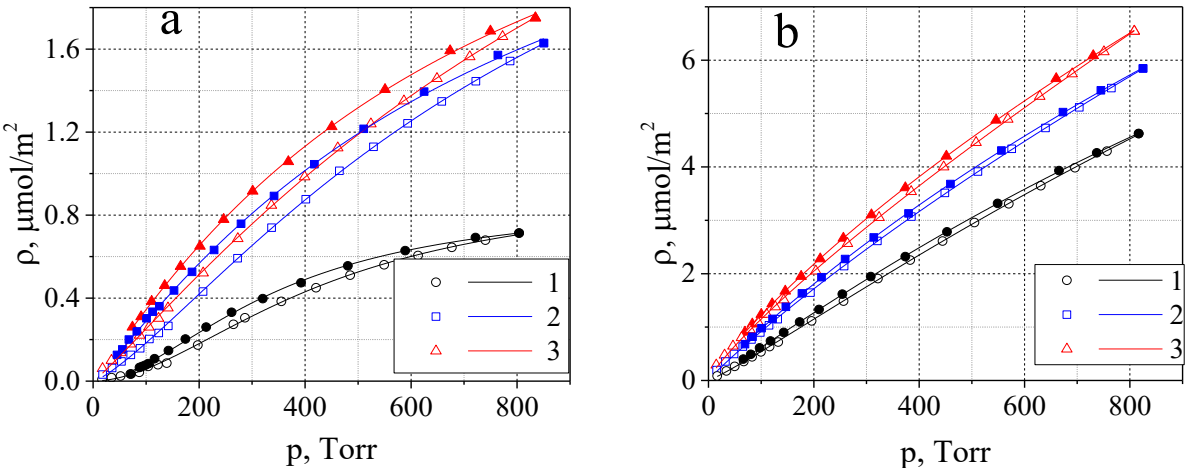

Fig. 8 – Adsorption of H_2 (1), N_2 (2), CO (3) over SiC-bulk-sucr at 253 K (8a, $|\Delta\mu_o|$ kJ/mol: 4.5 (1a); 5.4 (2a); 5.8 (3a)) and 197 K (8b, $|\Delta\mu_o|$ kJ/mol: 4.3 (1b); 4.9 (2b); 5.2 (3b)). Filled symbols – adsorption, empty symbols – desorption. Symbols correspond to experimental data while lines correspond to calculations according to eq. 1.

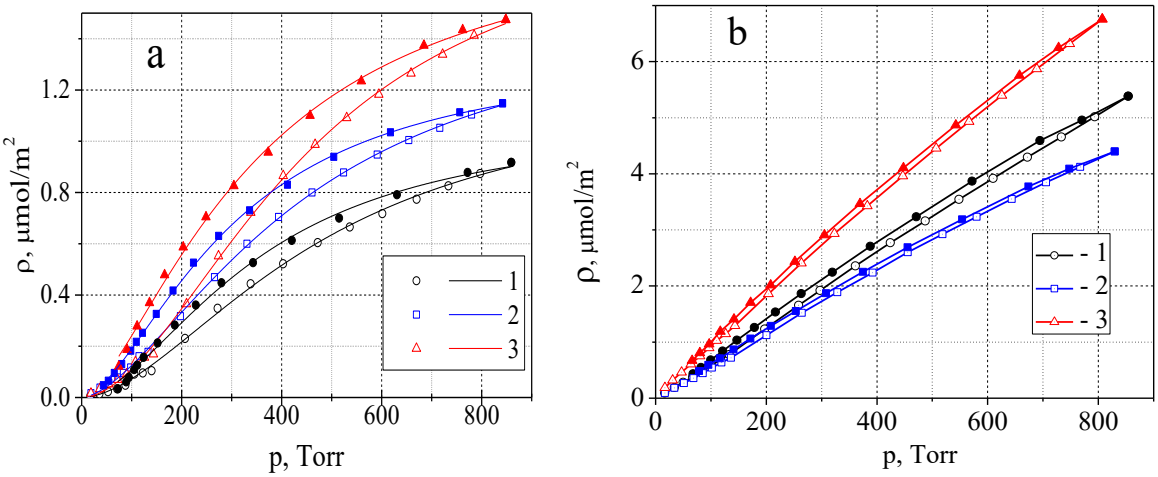

Fig. 9 – Adsorption of H_2 (1), N_2 (2), CO (3) over C_3N_4 at 253 K (9a, $|\Delta\mu_o|$ kJ/mol: 4.6 (1a); 5.0 (2a); 4.7 (3a)) and 197 K (9b, $|\Delta\mu_o|$ kJ/mol: 4.3 (1b); 4.5 (2b); 4.7 (3b)). Filled symbols – adsorption, empty symbols – desorption. Symbols in Fig. 9a correspond to experimental data while lines correspond to calculations according to eq. 1.

As can be seen from Figs. 8 and 9 the calculated adsorption isotherms are in a good agreement with experimental results for both adsorption and desorption.

The values of the parameter α_2 (Table 4) reflect deviations from linearity. Analysis of Table 4 shows that this parameter gives the largest deviation from linearity for CO adsorption followed by H_2 adsorption which can be due to accelerated interactions of adsorbates with the adsorbent in the former case.

Table 4 – The parameters calculated using the Sips equation (1). The errors in parameters are lower than ca. 20% if not otherwise stated.

Sample	Adsorbate (T, K)	α_1 for adsorption, in parenthesis for desorption	α_2 for adsorption, in parenthesis for desorption	α_3 for adsorption, in parenthesis for desorption
SiC-bulk-sucr	H_2 (253 K)	0.94 (0.87)	1.83 (1.80)	67395 (38590)
	N_2 (253 K)	3.40 (3.13)	1.30 (1.12)	6814 (1680)
	CO (253 K)	4.58 (3.30)	1.12 (1.09)	2913 (1251)
	H_2 (197 K)	21.28 (17.65)	1.12 (1.08)	6679 (4048)
	N_2 (197 K)	52.35 (28.77)	0.92 (0.95)	3950 (2231)
	CO (197 K)	n.r.* (47.50)	0.83 (0.86)	n.r.* (2000)
C_3N_4	H_2 (253 K)	1.22 (1.09)	1.76 (1.77)	51085** (32971**)
	N_2 (253 K)	1.53 (1.35)	1.64 (1.64)	21024 (11755)
	CO (253 K)	1.92 (1.85)	1.85 (1.52)	80832** (7380**)
SiC-bulk-sucr-HF	H_2 (253 K)	0.38	1.62	25672**
	N_2 (253 K)	0.75	1.39	11444
	CO (253 K)	3.84 (3.84)	1.71 (1.51)	55730 (13306)

* n.r. not reliable due to large errors, exceeding 100%; ** errors between 25 and 50%.

A similar cooperative adsorption behavior was observed for other gases in the supercritical temperature range (197 – 273 K). Upon adsorption of hydrogen, nitrogen and carbon monoxide under the same conditions on the surface of SiC-bulk-sucr, the specific adsorption at 760 Torr was respectively 0.6, 1.5 and 1.7 μmol/m^2 at adsorption energies of 4.5, 5.4 and 5.8 kJ/mol. For SiC-bulk-sucr-HF – coating for the same gases, the corresponding values are respectively 0.3, 0.35 and 2.4 μmol/m^2 at the energy of 4.7, 4.9 and 4.9 kJ/mol. With a decrease in temperature to 197 K, adsorption energy of these gases on SiC-bulk-sucr-HF (Fig. 10) is decreased unexpectedly to 4.4 kJ/mol for all gases (H_2, N_2, CO). Coating substantially elevated adsorption up to 10 – 11 μmol/m^2, which is a sign

of cooperative adsorption, accompanied by changes in the interactions of gases with semiconductor surfaces. Experimental data for adsorption and desorption of hydrogen and nitrogen did not show any hysteresis thus the values of parameters are the same for both branches. For modelling of experimental data in the case of CO adsorption and desorption the parameter α_1 was set to be the same as it reflects the maximum loading. As expected the calculated value of α_2 is lower for desorption as the S-shaped behavior is less pronounced.

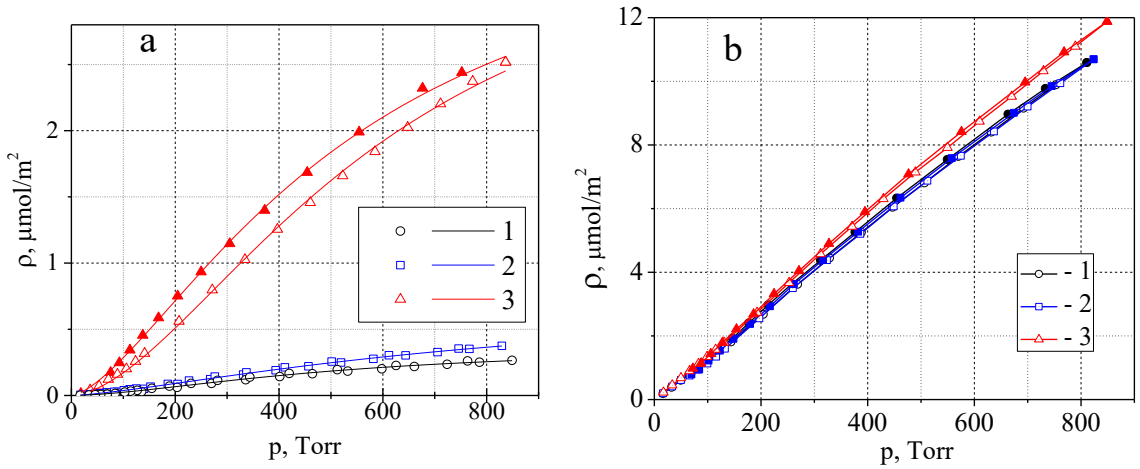

Fig. 10 – Adsorption of H_2 (1), N_2 (2), CO (3) over SiC-bulk-sucr-HF at 253 K (10a, $|\Delta\mu_o|$ kJ/mol: 4.7 (1a); 4.9 (2a); 4.9 (3a)) and 197 K (10b, $|\Delta\mu_o|$ kJ/mol: 4.4 (1b); 4.4 (2b); 4.4 (3b)). Symbols in Fig. 10a correspond to experimental data while lines correspond to calculations according to eq. 1.

In the investigated series of gases, the nature of the adsorbate, namely the dipole, quadrupole moments and polarization ability, determining the energy and the level of adsorption [41], did not influence adsorption on some SiC semiconductors such as SiC-nanoamor (Fig. 11). For this case, displaying unusually high loadings in the supercritical temperature range at low levels of adsorption energy, no differences for the studied gases were seen. For SiC-bulk-sucr acceleration of adsorption is barely noticeable. At 197 K behavior of H_2, N_2 and CO was similar for other materials (adsorption energies, respectively, – 4.3, 4.9 and 5.2 kJ/mol and the level of specific adsorption – 4.5, 5.8 and 6.5 μmol/m^2).

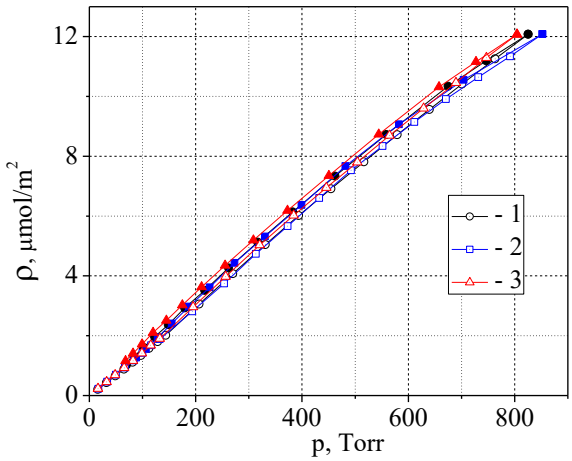

Fig. 11 – Adsorption of H_2 (1), N_2 (2), CO (3) over SiC-nanoamor at 197 K ($|\Delta\mu_o|$ kJ/mol: 4.3 (1); 4.3 (2); 4.3 (3)).

Enhanced adsorption was also manifested in case of CO_2 on SiC. Namely, the specific adsorption in the supercritical temperature region (253 K, 760 Torr) for carbon (CMK-1) is 3.2 μmol/m^2 at the energy of 9.1 kJ/mol, while for SiC-bulk-sucr and SiC-bulk-sucr-HF under the same conditions, the corresponding values are 4.2 and 5.2 μmol/m^2 at the energy levels of 8.9 and 6.5 kJ/mol, respectively (Table 5). Higher levels of CO_2 adsorption over SiC samples in comparison with other studied gases and absence of noticeable differences in adsorption on the surface of different nature (C, SiC and C_3N_4) can be explained by significant differences in physical properties determining the level of intermolecular interactions ($T_{crit.CO2}$ = 197 K) [41].

Table 5 – Adsorption of carbon dioxide (T = 197, 253, 273 K) over carbon nitride, silicon carbide and carbon obtained by bulk and template methods.

Sample	Adsorption of CO_2 at 760 Torr					
	Specific adsorption on the surface, μmol/m^2			Adsorption potential $\|\Delta\mu_o\|$, kJ/mol		
	197 K	253 K	273 K	197 K	253 K	273 K

CMK-1	15.2	5.4	3.0	11.9	9.0	8.6
C_3N_4-bulk	14.60	4.89	3.43	9.1	10.3	9.9
CN-SBA-15	13.38	4.07	3.58	8.0	8.1	7.8
SiC-bulk-sucr	12.43	4.91	3.27	11.0	8.9	9.3
SiC-bulk-sucr-HF	13.92	4.83	3.03	8.3	6.5	6.5

5. Conclusions

A comparative study of hydrogen adsorption over silicon carbide materials of different nature was performed. An increase of hydrogen adsorption for silicon carbide compared with adsorbents of another nature (silica, carbon) is apparently associated with appearance of dipole interactions and, to a larger extent, a cooperative nature of adsorption on semiconductor surfaces when novel adsorption sites are generated during exposure to the adsorbate. Unusually high values of specific hydrogen adsorption (up to 15 μmol/m^2) for silicon carbide obtained by the template method in comparison with the traditional bulk method and highly crystalline commercial SiC were observed. For such SiC materials the highest specific hydrogen adsorption was associated with a more perfect truly "carbide" structure with a higher content of Si–C bonds in the form of carbide. However, for high specific hydrogen adsorption, some non-stoichiometricity is required, which is related to presence of carbon in other (non-carbide) bonds (graphite or terminal and sp^3 hybridized C). The influence of the adsorbate nature for a number of gases (H_2, N_2, CO) was less prominent (or absent) for templated silicon carbide compared to carbon and silica materials. Cooperative behavior of hydrogen adsorption in the case of SiC was accompanied by an abnormally high loading of the adsorbent surface in the supercritical region.

References

[1] Froudakis GE. Hydrogen storage in nanotubes & nanostructures. Mater Today 2011;14:324–328. https://doi.org/10.1016/S1369-7021(11)70162-6.

[2] Dutta S. A review on production, storage of hydrogen and its utilization as an energy resource. J Ind Eng Chem 2014;20:1148–1156. https://doi.org/10.1016/j.jiec.2013.07.037.

[3] Wang P, Orimo S, Matsushima T, Fujii H, Majer G. Hydrogen in mechanically prepared nanostructured h-BN: a critical comparison with that in nanostructured graphite. Appl Phys Lett 2002;80:318–320. https://doi.org/10.1063/1.1432447.

[4] Tang C, Bando Y, Ding X, Qi S, Golberg D. Catalyzed collapse and enhanced hydrogen storage of BN nanotubes. J Am Chem Soc 2002;124:14550–14551. DOI: 10.1021/ja028051e.

[5] Pham-Huu C, Keller N, Ehret G, Ledoux MJ. The first preparation of silicon carbide nanotubes by shape memory synthesis and their catalytic potential. J Catal 2001;200:400–410. https://doi.org/10.1006/jcat.2001.3216.

[6] Sun XH, Li CP, Wong WK, Wong NB, Lee CS, Lee ST et al. Formation of silicon carbide nanotubes and nanowires via reaction of silicon (from disproportionation of silicon monoxide) with carbon nanotubes. J Am Chem Soc 2002;124:14464–14471. DOI: 10.1021/ja0273997.

[7] Mpourmpakis G, Froudakis GE, Lithoxoos GP, Samios J. SiC nanotubes: a novel material for hydrogen storage. Nano Lett 2006;6:1581–1583. DOI: 10.1021/nl0603911.

[8] Barghi SH, Tsotsis TT, Sahimi M. Hydrogen sorption hysteresis and superior storage capacity of silicon-carbide nanotubes over their carbon counterparts. Int J Hydrogen Energy 2014;39:21107–21115. https://doi.org/10.1016/j.ijhydene.2014.10.087.

[9] He RA, Chu ZY, Li XD, Si YM. Synthesis and hydrogen storage capacity of SiC nanotube. Key Eng Mater 2008; 368:647–649. https://doi.org/10.4028/www.scientific.net/KEM.368-372.647.

[10] Barghi SH, Tsotsis TT, Sahimi M. Experimental investigation of hydrogen adsorption in doped silicon-carbide nanotubes. Int J Hydrogen Energy 2016;41:369–374. https://doi.org/10.1016/j.ijhydene.2015.10.091.

[11] Shcherban ND, Filonenko SM, Yaremov PS, Sergiienko SA, Ilyin VG, Murzin DYu. Carbothermal synthesis of porous silicon carbide using mesoporous silicas. J Mater Sci 2017;52:3917-3926. https://doi.org/10.1007/s10853-016-0652-7.

[12] Wang X, Liew KM. Hydrogen storage in silicon carbide nanotubes by lithium doping. J Phys Chem C 2011;115:3491–3496. DOI: 10.1021/jp106509g.

[13] Mahdizadeh SJ, Goharshadi EK. Hydrogen storage on silicon, carbon, and silicon carbide nanotubes: A combined quantum mechanics and grand canonical Monte Carlo simulation study. Int J Hydrogen Energy 2014;39:1719–1731. https://doi.org/10.1016/j.ijhydene.2013.11.037.

[14] Singh RS, Solanki A. Hydrogen adsorption in metal-decorated silicon carbide nanotubes. Chem Phys Lett 2016;660:155–159. https://doi.org/10.1016/j.cplett.2016.08.021.

[15] Wolkenstein FF. Electron phenomena in adsorption and catalysis on semiconductors (in Russian). Moscow: Mir; 1969.

[16] Rhodes RG. Imperfections and active centers in semiconductors (in Russian). Moscow: Metallurgy; 1968.

[17] Wolkenstein FF. Physical chemistry of semiconductor surface (in Russian); Moscow: Nauka; 1973.

[18] Ledoux MJ, Pham-Huu C. Silicon carbide: a novel catalyst support for heterogeneous catalysis. Cattech 2001;5:226–246. https://doi.org/10.1023/A:1014092930183.

[19] Shcherban ND. Review on synthesis, structure, physical and chemical properties and functional characteristics of porous silicon carbide. J Ind Eng Chem 2017;50:15–28. https://doi.org/10.1016/j.jiec.2017.02.002.

[20] Zhao D, Feng J, Huo Q, Melosh N, Fredrickson GH, Chmelka BF et al. Triblock copolymer syntheses of mesoporous silica with periodic 50 to 300 angstrom pores. Science 1998;279:548–552. DOI: 10.1126/science.279.5350.548.

[21] Zhao YC, Yu DL, Zhou HW, Tian YJ, Yanagisawa O. Turbostratic carbon nitride prepared by pyrolysis of melamine. J Mater Sci 2005;40:2645–2747. https://doi.org/10.1007/s10853-005-2096-3.

[22] Li Q, Yang J, Feng D, Wu Z, Wu Q, Park SS et al. Facile synthesis of porous carbon nitride spheres with hierarchical three-dimensional mesostructures for CO_2 capture. Nano Res 2010;3:632–642. https://doi.org/10.1007/s12274-010-0023-7.

[23] Gregg SG, Sing KSW. Adsorption, surface area and porosity. New York: Academic Press; 1982.

[24] Barrett EP, Joyner LG, Halenda PP. The determination of pore volume and area distributions in porous substances. I. Computations from nitrogen isotherms. J Am Chem Soc 1951:73:373–380. DOI: 10.1021/ja01145a126.

[25] Adolphs J. Excess surface work—A modelless way of getting surface energies and specific surface areas directly from sorption isotherms. Appl Surf Sci 2007;253:5645–5649. https://doi.org/10.1016/j.apsusc.2006.12.089.

[26] Alekseev S, Shamatulskaya E, Volvach M, Gryn S, Korytko D, Bezverkhyy I, et al. Size and surface chemistry tuning of silicon carbide nanoparticles. Langmuir 2017; 33:13561–13571. DOI: 10.1021/acs.langmuir.7b02784.

[27] Shcherban N, Filonenko S, Sergiienko S, Yaremov P, Skoryk M, Ilyin V, et al. Morphological features of porous silicon carbide obtained via a carbothermal method. Int J Appl Ceram Tec 2018;15:36–41. https://doi.org/10.1111/ijac.12757.

[28] Wu IJ, Guo GY. Optical properties of SiC nanotubes: an ab initio study. Phys Rev B 2007;76:035343. https://doi.org/10.1103/PhysRevB.76.035343.

[29] Froudakis GE. Why alkali-metal-doped carbon nanotubes possess high hydrogen uptake. Nano Let 2001;1:531–533. DOI: 10.1021/nl0155983.

[30] Peng X, Krüger P, Pollmann J. Metallization of the 3 C− Si C (001)−(3× 2) surface induced by hydrogen adsorption: A first-principles investigation. Phys Rev B 2005;72:245320. https://doi.org/10.1103/PhysRevB.72.245320.

[31] Oura K, Lifshits VG, Saranin AA, Zotov AV, Katayama M. Hydrogen interaction with clean and modified silicon surfaces. Surf Sci Rep 1999;35:1–69. https://doi.org/10.1016/S0167-5729(99)00005-9.

[32] Boland JJ. Structure of the H-saturated Si (100) surface. Phys Rev Lett 1990;65:3325. https://doi.org/10.1103/PhysRevLett.65.3325.

[33] Van Bommel AJ, Crombeen JE, Van Tooren A. LEED and Auger electron observations of the SiC (0001) surface. Surf Sci 1975;48:463–472. https://doi.org/10.1016/0039-6028(75)90419-7.

[34] Chang CS, Tsong IST, Wang YC, Davis RF. Scanning tunneling microscopy and spectroscopy of cubic β-SiC (111) surfaces. Surf Sci 1991;256:354–360. https://doi.org/10.1016/0039-6028(91)90877-U.

[35] Johansson LI, Owman F, Mårtensson P. High-resolution core-level study of 6H-SiC (0001). Phys Rev B 1996; 53:13793. https://doi.org/10.1103/PhysRevB.53.13793.

[36] Taylor TN. The surface composition of silicon carbide powders and whiskers: An XPS study. J Mater Res 1989;4:189–203. https://doi.org/10.1557/JMR.1989.0189.

[37] Lianos L, Berthet A, Deranlot C, Aires FCS, Massardier J, Bertolini JC. Catalytic properties of Pd deposited on SiC (0001) single crystal surfaces. J Catal 1998;177:129–136. https://doi.org/10.1006/jcat.1998.2063.

[38] Xie W, Möbus G, Zhang S. Molten salt synthesis of silicon carbide nanorods using carbon nanotubes as templates. J Mater Chem 2011;21:18325–18330. DOI:10.1039/C1JM13186A.

[39] Sips R. On the structure of a catalyst surface. J Chem Phys 1948;16:490–495. https://doi.org/10.1063/1.1746922.

[40] Foo KY, Hameed BH. Insights into the modeling of adsorption isotherm systems. Chem Eng J 2010;156:2–10. https://doi.org/10.1016/j.cej.2009.09.013.

[41] Yaremov PS, Scherban ND, Ilyin VG. Adsorption of nitrogen, hydrogen, methane, and carbon oxides on micro- and mesoporous molecular sieves of different nature. Theor Exp Chem 2013;48:394–400. https://doi.org/10.1007/s11237-013-9287-9.